

2018

Condensation heat transfer of R22, R410A and R32 inside a multiport mini-channel tube

Pham-Quang Vu

Graduate School, Chonnam National University, San 96-1, Dunduk-Dong, Yeosu, Chonnam 550-749, Republic of Korea,
phamquangvu911273@gmail.com

Kwang-Il Choi

Department of Refrigeration and Air Conditioning Engineering, Chonnam National University, San 96-1, Dunduk-Dong, Yeosu, Chonnam 550-749, Republic of Korea, imcgi@chonnam.ac.kr

Jong-Taek Oh

ohjt@chonnam.ac.kr

Honggi Cho

Advanced R&D Team, Digital Appliances, Samsung Electronics, Korea, Republic of (South Korea),
honggi.cho@samsung.com

Follow this and additional works at: <https://docs.lib.purdue.edu/iracc>

Vu, Pham-Quang; Choi, Kwang-Il; Oh, Jong-Taek; and Cho, Honggi, "Condensation heat transfer of R22, R410A and R32 inside a multiport mini-channel tube" (2018). *International Refrigeration and Air Conditioning Conference*. Paper 1914.
<https://docs.lib.purdue.edu/iracc/1914>

This document has been made available through Purdue e-Pubs, a service of the Purdue University Libraries. Please contact epubs@purdue.edu for additional information.

Complete proceedings may be acquired in print and on CD-ROM directly from the Ray W. Herrick Laboratories at <https://engineering.purdue.edu/Herrick/Events/orderlit.html>

Condensation heat transfer of R22, R410A and R32 inside a multiport mini-channel tube

Quang Vu PHAM¹, Kwang-Il CHOI², Jong-Taek OH^{2*}, Honggi CHO³

¹Graduated school, Department of refrigeration and Air Conditioning Engineering, Chonnam National University, 50 Daehak-ro, Yeosu, Chonnam, 59626, Korea.
(82-10-8688-4767, phamquangvu911273@gmail.com)

²Department of Refrigeration and Air Conditioning Engineering, Chonnam National University, 50 Daehak-ro, Yeosu, Chonnam, 59626, Korea.
(82-61-659-7273, 82-61-659-7279, ohjt@chonnam.ac.kr)

³Advanced R&D Team, Digital Appliances, Samsung Electronics, 129 Samsung-ro, Yeongtong-gu Suwon, 16677, Republic of Korea.

ABSTRACT

In the present study, the heat transfer coefficients are investigated experimentally for the flow condensation of R22, R410A, and R32 inside a horizontal multiport rectangular mini-channel tube. The multiport tube has nine channels with the hydraulic diameter of 0.969 mm. The experimental measurements were carried out at the fixed saturation temperature of 48°C, by the varying refrigerant mass flux from 50 to 500kg/m²s, and the heat flux range from 3 to 15kW/m². The effects of vapor quality, mass flux and heat flux on condensation characteristics is are clarified. The experiment results were compared with the existing heat transfer coefficient correlations developed for condensation in multiport mini-channel. A new correlation was proposed using the present data with good prediction.

1. INTRODUCTION

Following the agreement of Montreal Protocol (1987) on progressive phase-out obligations in developed and developing countries for all the major ozone-depleting substance, including CFCs, halons, and less damaging transitional chemicals such as HCFCs, in 1997, the Kyoto Protocol implemented the objective of the United Nations Framework Convention on Climate Change to fight global warming by reducing greenhouse gas concentrations in the atmosphere to a level that would prevent dangerous anthropogenic interference with the climate system. Therefore, a serious consideration of global warming effect should be made for developing a new refrigerant. Near-azeotropic refrigerant mixture R410A is chosen to replace R22 in current stage owing to zero ozone depletion potential (ODP), offer higher efficiency, lower energy costs. However, the high global warming potential of R410A may not be suitable in future. In 1990, R32 was chosen as the alternative refrigerant for R22, but was eventually removed due to its flammability. R32 was only used as a component of refrigerant mixtures. Nowadays, the current concerns and limitations about GWP have brought R32 to the attention of researchers as an alternative to R410A. R32 has similar pressure and compression ratio R410A, thus, allowing a close drop-in replacement without major system redesign. Also, the cooling capacity per unit volume of R32 is higher than that of R410A. With good thermal performance and environmental characteristics, R32 has become a highly promising alternative refrigerant in Japan, China, and some Asia countries. The comparison of properties of R410A, R22, and R32 is given in Table 1.

On the other hand, in the automotive air-conditioning, heat pump and some other industrial applications, the multiport mini/micro channel tubes are increasingly used to improve the heat transfer coefficient, enhance compactness of heat exchanger, and to reduce air side pressure and substantial the refrigerant charge.

A number of research works focus on the condensation heat transfer coefficient of R410A, R22 and R32 in mini/micro horizontal tube. Jige et al. (2016) investigated the condensation heat transfer and pressure drop characteristic of R134a, R32, R1234ze(E) and R410A in a horizontal multi-port tube. The authors concluded that the frictional pressure drop of R1234ze(E) is higher than that of R134a, R32 and R40A by the magnitude relationships of the vapor density and liquid viscosity. Moreover, the effect of the surface tension is dominated at the low mass flux for a wide vapor quality range on the condensation process inside rectangular channel. López-Belchí et al. (2017, 2016) compared the heat transfer performance of condenser based on mini-channels with R410A and R32 as working fluids. They reported that the R32 presents higher latent heat, heat transfer coefficient and pressure drop than R410A, for a specifically designed system for R32 or modified to operate with R32 the refrigerant charge will decrease, and the energy efficiency will increase, decreasing the environmental impact of system. Liu and Li (2016) demonstrated experimentally the pressure drop of R32, R152a and R22 during condensation in three types of horizontal mini-channels. They reported that pressure drops of R32 are almost equal to those for R22, and R152a are good substitutes for R22 in smaller friction pressure drop during condensation.

Wang & Rose (2005) presented work on the condensation in the horizontal square and triangular micro-channels with R134a, R22, and R410A as working fluids. The authors concluded that the heat transfer coefficient enhances significantly by the surface tension towards the channel entrance. Also, the heat transfer coefficient of R22 and R134a are almost the same whereas those for R410A are somewhat smaller.

However, the comparison of condensation heat transfer coefficient of R410A, R22, and R32 inside multiport mini-channel tube still lack in the open literature. Therefore, the experimental condensation heat transfer coefficients of R410A, R22 and R32 inside multiport rectangular mini-channels have been reported in this study. The influence of mass flux, heat flux and vapor quality is analyzed and a new correlation for heat transfer coefficient is also proposed.

2. EXPERIMENTAL APPARATUS

As schematically shown in figure 1, the experimental setup consists of two independent loops, namely, the refrigerant loop containing the test section, and the water cooling loop. The refrigerant loop consists of a liquid receiver, a micro gear pump, a sub-cooling, a Coriolis mass flow meter, a pre-heater, a test section, and a condenser. In order to control the mass flow rate of refrigerant flowing into the system, micro gear pump is connected to a speed controller. The saturation temperature and vapor quality of refrigerant at the inlet of the test section are

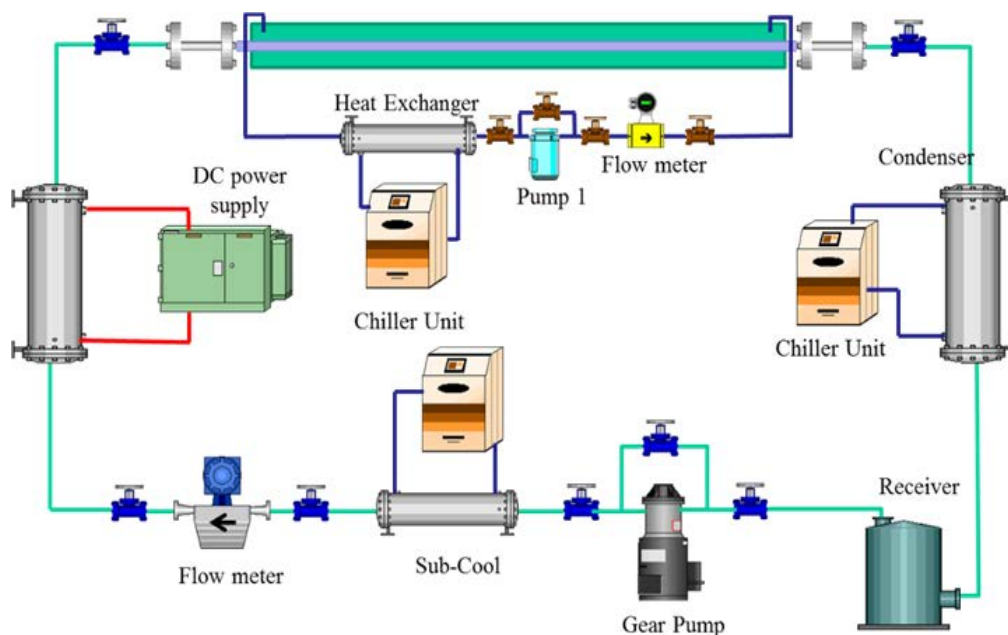


Figure 1: Schematic diagram of experimental apparatus

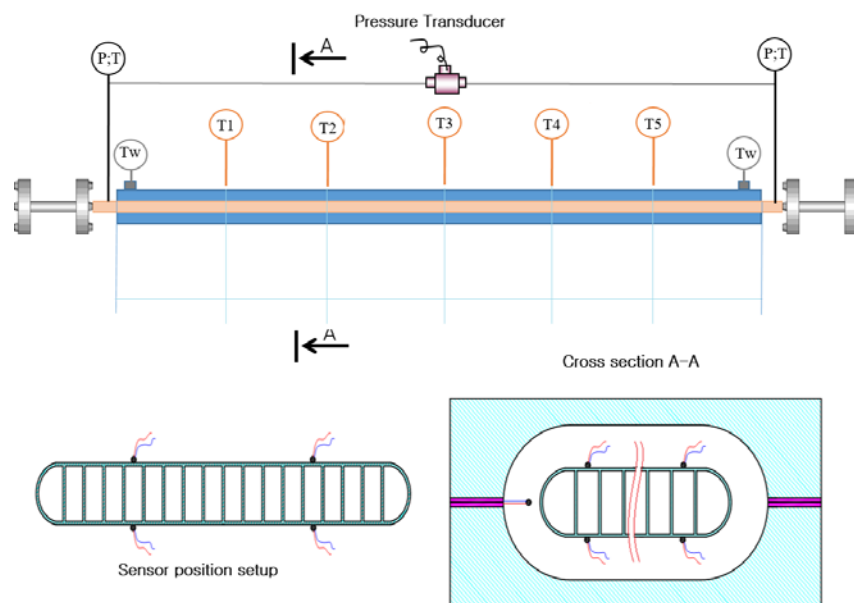


Figure 2: Detail of test section

adjusted by an electric pre-heater.

The test section is the main component of the refrigerant loop. As shown in the cross section in Fig. 2, it is made as a tube-in-tube heat exchanger. The inner tube is a multiport mini-channel tube. The outer tube was made of acrylic with the gap size of 1 mm and has the same profile with test tube. The test section constructed for this study is designed to condense refrigerant by rejecting heat to cooling water flowing in annulus side. The temperatures of the cooling water at the inlet and outlet of the test section is measured by two RTDs. The mass flow rate is also measured by another Coriolis mass flow meter. The wall temperature of the test section is measured in three points located along of test section by means of T-type thermocouples. Three absolute pressure transducers and two differential pressure transducers are connected to the inlet of pre-heater, inlet and outlet of the test section to measure the local pressure as well as pressure drop. Finally, the two-phase mixture that leaves the test section is completely condensed in another heat exchanger thanks to the cold water provided by the cooling water bath. The sub cooled refrigerant from the condenser is then returned to a liquid receiver tank from which the cycle will be repeated. A control system is also deployed to guarantees the steady state of working system and ensures that all measurements are properly made.

3. MEASUREMENTS, DATA PROCESSING AND ERROR ANALYSIS

Twenty T-types thermocouple 0.13mm diameter were attached at 5 positions along the test section tubes. At each position, the tube wall temperature is measured at both top and bottom sides as described in cross section view in Fig.2. The high accuracy RTDs class-A with 3-wires, 100-ohm Platinum type is used to measure the temperatures of refrigerant and cooling water. Both thermocouples and resistance temperature detectors were preliminary calibrated using the Azonix digital RTD thermometer. The resulting standard deviation is of 0.1K for the T-type thermocouples, and of 0.01K for the RTDs. The refrigerant pressure and temperature at the inlet of pre-heater are

Table 1 Physical properties of refrigerant

Refrigerant	Liquid dens. (kg/m ³)	Vapor dens. (kg/m ³)	Liquid Visc. (μPa.s)	Vapor Visc. (μPa.s)	Latent heat (kJ/kg)	Ther. Cond. (mW/mk)	Sur. Tens. (N/m)	GWP
R410A	921.7	132.3	84.6	15.8	140.9	76.71	0.0023	2088
R32	851	92.8	85.5	14.5	215.5	108.5	0.0033	675
R22	1091	81.5	126	13.6	157	72.8	0.0049	1700

measured by a pressure sensor and a RTD class-A sensor to define inlet state of refrigerant. A pressure sensor was installed at the inlet of test section to measure the saturation pressure for refrigerant. Also that pressure used to indirectly calculate the saturation temperature of refrigerant before entering the test section. All absolute pressure transducers were calibrated with an accuracy of $\pm 0.02\%$ of full scale and a maximum error of ± 0.7 kPa. Two Coriolis mass flow meters were used to measure the refrigerant and cooling water mass flow rate with a precision of 0.05%. The reliability of energy balance is verified by initial testing with single phase flow heat transfer of water-

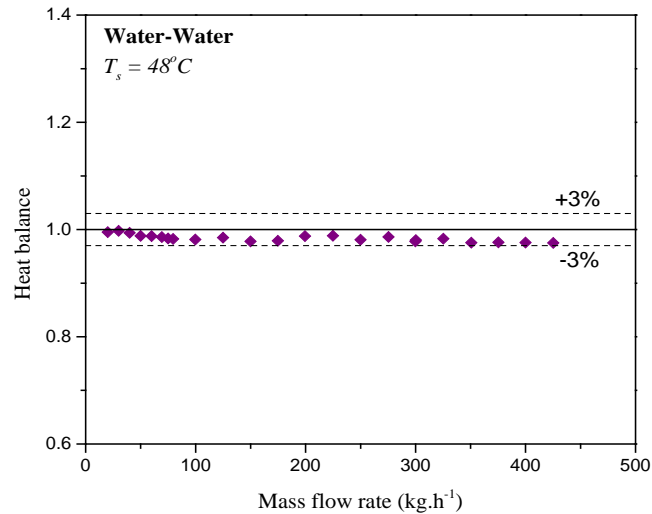


Figure 3: Energy balance in test sections

water in test section, the error of heat balance between the cooling water side and inside hot fluid was always less than $\pm 3\%$. The energy balance between two side fluids in the preliminary test shown in Figure 3. For each experimental case, the experiment model has kept stability in 30 minutes before taking data in 10 minute periods. The experiment processing has been repeated in some random experimental cases on two different days, by measuring the heat transfer coefficient for the same experimental conditions. The difference between the times of the verification is acceptable within about 6% of maximum difference. The experimental data was measured in a steady-state condition during the experimental process. The uncertainty of the experimental results was determined by the procedure proposed by Moffat (Moffat, 1988). The uncertainty of the measured and calculated parameters are listed in Table 1.

The experiments of the R410A, R32 and R22 condensing flow in the test section were carried out at a fixed condensation temperature of 48°C, 50-500 kg.m⁻².s⁻¹ of mass flux and 3-15 kW.m⁻² of heat flux. The data reduction in the measured results is summarized in the following procedures. The vapor quality at the inlet of the test section was controlled by a DC power supply and can be determined as follows:

$$x_{inlet} = \frac{1}{h_{fg}} \left[\frac{Q_{pre}}{m_{ref}} - C_p (T_{sat} - T_{p,inlet}) \right] \quad (1)$$

where Q_{pre} is the heating power applied in the pre-heater by the DC power supply unit. The saturation temperature T_{sat} was computed from the measured saturation pressure at the inlet of the test section. The average heat flux in the test section was determined as:

$$q = \frac{m_{water} c_{p,water} \Delta T_{water}}{A_{external}} \quad (2)$$

where m_{water} is the cooling water mass flow rate, ΔT_{water} is the temperature difference between the inlet and outlet of the cooling water side, and $A_{external}$ is the external surface area of the test section tube. The cooling water mass flow rate in all cases is fixed at 1kg/min to maintain the water flow distribution on the annulus side. Two test section lengths were used with different mass flux conditions to control the vapor quality difference in the test section

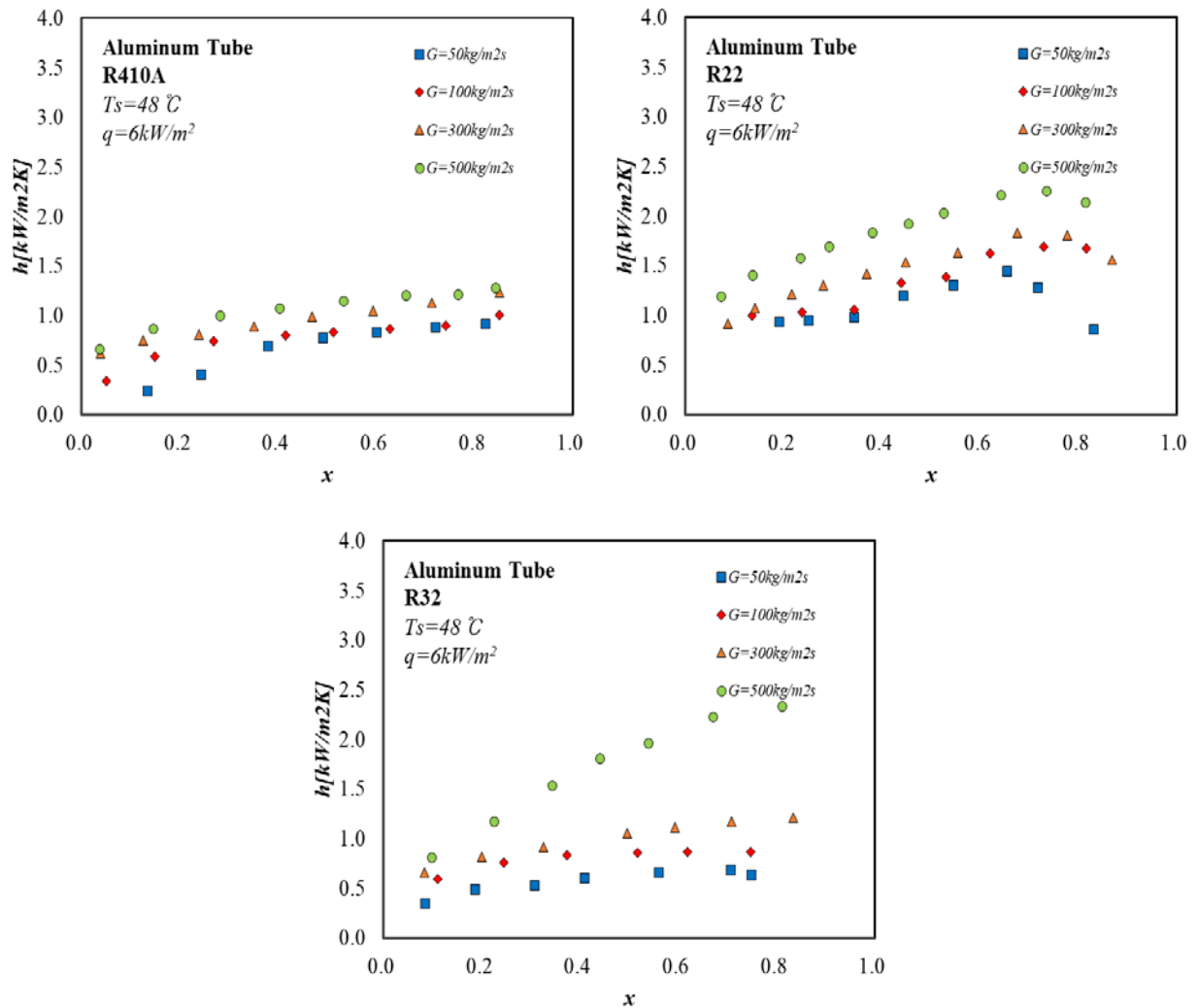


Figure 4: Effect of mass flux on the heat transfer coefficient

approximately 0.011-0.16. Therefore, it can be assumed that the variation in vapor quality on the test section is linear over the length of test section. The vapor quality in the test section is calculated by the following equation (3):

$$x = x_{inlet} - \frac{m_{water} c_{p,water} \Delta T_{water}}{2m_{ref} h_{fg}} \quad (3)$$

The average condensation heat transfer coefficient is obtained as:

$$h = \frac{A_{external}}{A_{internal}} \frac{q}{(T_{sat} - T_{w,i})} \quad (4)$$

$T_{w,i}$ is the inside surface wall temperature, in which each temperature point is calculated from the measured outside wall temperature using the Fourier steady-state one-dimensional heat conduction method. The physical properties in the data reduction of each experiment were calculated using REFPROP version 8.0.

4. RESULTS AND DISCUSSION

The experiments were made over a wide range of test conditions. The influence of variable mass flux, heat flux, vapor quality on the heat transfer coefficient was investigated. Fig. 4 depicted the heat transfer coefficient versus vapor quality and mass flux of R410A, R22 and R32. The effect of varying mass flux can be clearly observed.

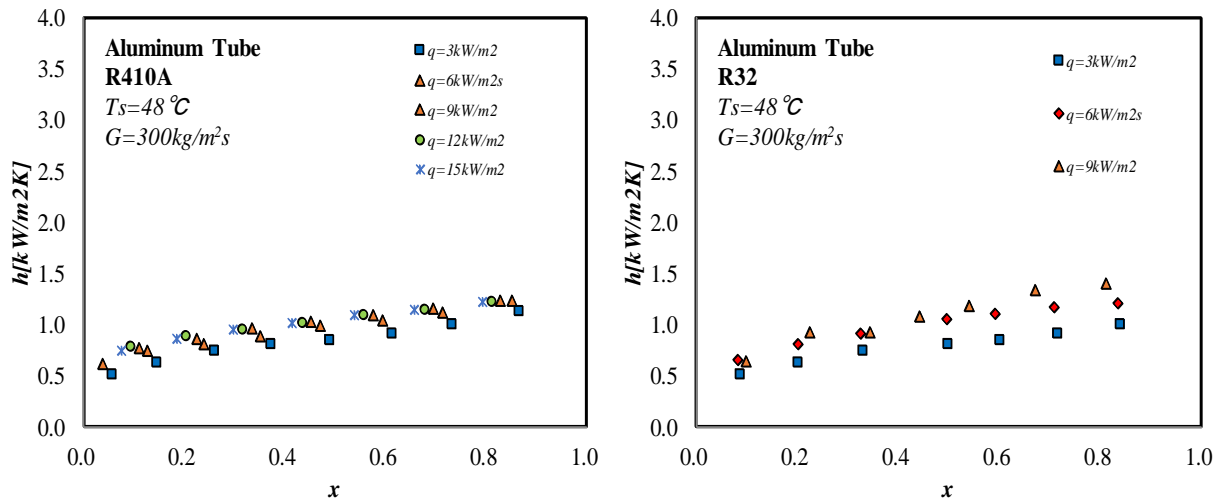


Figure 5: Effect of heat flux on the heat transfer coefficient

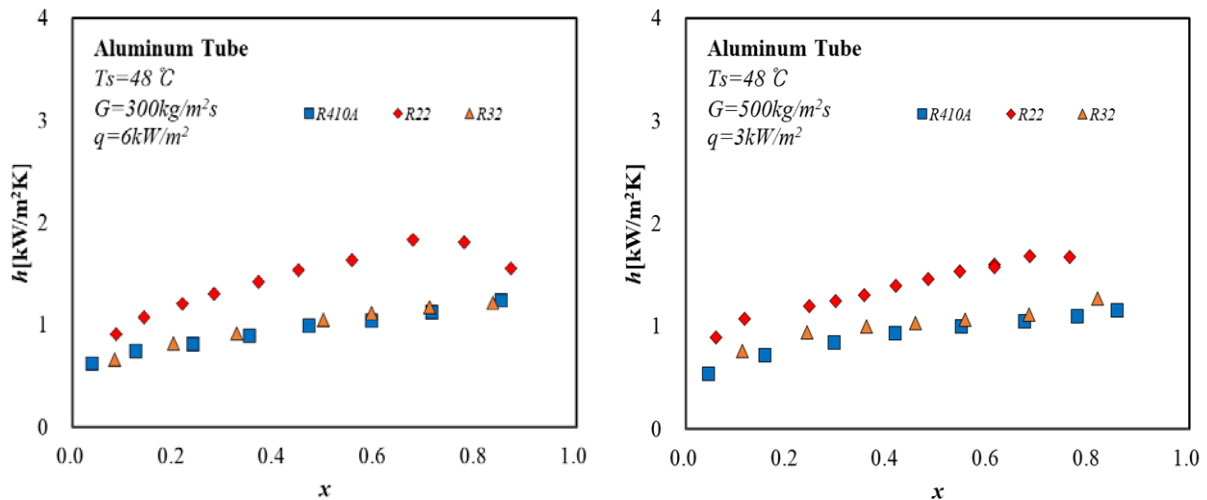


Figure 6: Comparison of heat transfer coefficient between three refrigerants

Condensation heat transfer coefficient increases with increasing of mass flux for three different refrigerants. The velocities of vapor and liquid phase become higher at high vapor quality, so more turbulence occurred between the surface of liquid film and vapor phase, which is the main reason for the increment of h_1 the heat transfer coefficient. However, the heat transfer coefficient shows the little dependence on the mass flux at low qualities and low mass flux. The heat transfer coefficients depend on both surface tension and shear stress. The liquid film of condensation liquid drainage in the edges of rectangular mini-channels is thinner at the side of channels because of surface tension. The contributions of forced convective condensation heat transfer and shear stress effects are dominant at high mass flux. On the contrary, under the low mass flux conditions, the surface tension is dominated, and shear stress may be lessened. The heat transfer coefficients at high vapor quality regime are almost constant or decrease because the flow pattern lays mist flow.

The heat fluxes applied on the test section were controlled by controlling the differences of temperature between inlet and outlet of cooling water in annulus side, while the mass flow rate of water was kept constantly at 1kg/min for all testing conditions. Fig.5 shows the effect of average heat flux on the measured condensation heat transfer coefficient of R410A. We found that the heat transfer coefficients increase with increasing heat flux, this reflects that the vapor condensation rate can be enhanced by a smaller amount when compared with an increase in the temperature difference between the refrigerant and the cold water in the test section. This means that more

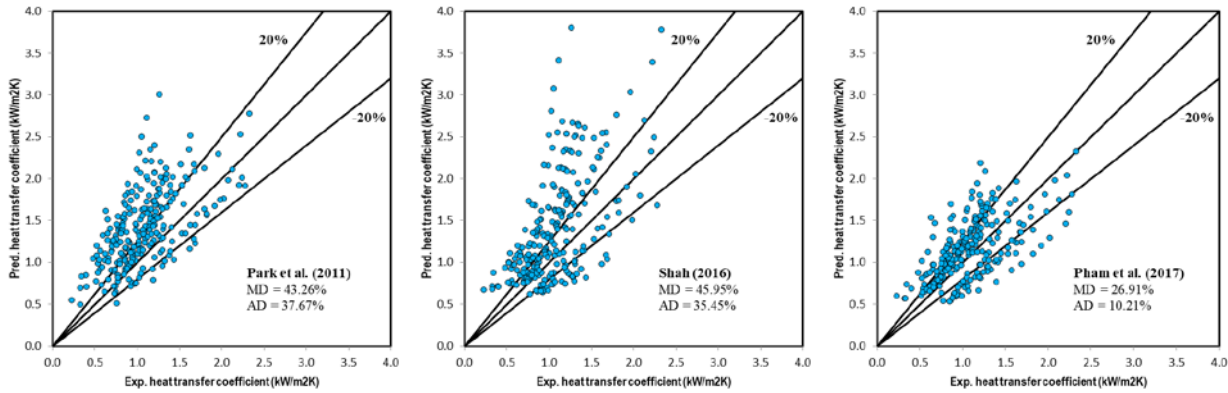


Figure 7: Comparison between existing correlation and present data

proportional control of the temperature gradient at the interface between the wall and the flow is needed to achieve a higher heat flux. Some studies (Zhang, Li, Liu, & Wang, 2012) investigated the condensation of R22, R410A and R407C inside mini-tubes, in which the authors reported that the heat transfer coefficient increases with increasing heat flux because of the effect of mass flux and heat flux on the interface temperature between the liquid film and bulk vapor. Furthermore, they concluded that the effect of heat flux on the heat transfer coefficient is more complicated for mixtures than for pure refrigerants.

The comparison of heat transfer coefficients among R410A, R22, and R32 is plotted in Fig. 6. The condensation heat transfer coefficients of R410A and R32 are relatively smaller than those for R22 at the same mass flux. The condensation heat transfer coefficients in the rectangular channel are also affected by the surface tension and liquid density. In rectangular channels, the liquid surface tension of R410A and R32 is about 53% and 32% lower than that of R22, so the condensed liquid film is well distributed on the surface resulting in an increase of the heat transfer coefficient. The liquid density of R22 is larger by 15% and 22% than that of R410A and R32 at 48°C, therefore, the condensed liquid at the upper side of the channel falls easily, which also increases the heat transfer coefficient. The heat transfer coefficient of R32 presents little higher than that of R410A because of its higher thermal conductivity. The flow pattern in mini-channels is mostly annular or intermittent, so liquid phase is displaced to the corners with the thin liquid film on the walls. The thin liquid film of R32 presents higher liquid thermal conductivity than R410A that leads to lower thermal resistance and higher heat transfer coefficient.

The experimental heat transfer coefficients were compared with some heat transfer coefficient correlations (M. M. Shah, 2016), (Park, Vakili-Farahani, Consolini, & Thome, 2011) and (Pham, Choi, Oh, & Cho, 2017) are illustrated in Fig. 7. The models of Shah (2016) and Park et al. (2011) do not give an accurate prediction with presented data. Main reason because it is not similar of the test conditions and the test tubes. (Pham et al., 2017) correlation shows the good agreement with experimental data with mean deviation about 26.9%. However, to improve the accuracy of heat transfer coefficient model, a modified correlation in the form proposed by (Pham et al., 2017) was developed from all the experimental data. The new correlation which considers the effect of channel geometry as the following equation:

$$h = 3.019Bo^{-0.517} Re_{eq}^{0.389} \left(\frac{1-x}{Pr_l} \right)^{0.262} \left((1-x)^{0.8} + \frac{x}{Pr_r} \right)^{0.1239} \left(\frac{q}{Gh_{lv}} \frac{A_{external}}{A_{internal}} \right)^{0.187} \left(\frac{\phi_v}{X_{tt}} \right)^{0.007} \frac{k_l}{d} \quad (5)$$

where the Bond number can be obtained as:

$$Bo = \frac{g(\rho_l - \rho_v)d^2}{\sigma} \quad (6)$$

The equivalent Reynolds number of the two-phase flow is given by

$$Re_{eq} = Re_l + \frac{\mu_v}{\mu_l} \left(\frac{\rho_l}{\rho_v} \right)^{0.5} Re_v \quad (7)$$

The two-phase pressure drop multiplier of the vapor flow is defined as the equation (8):

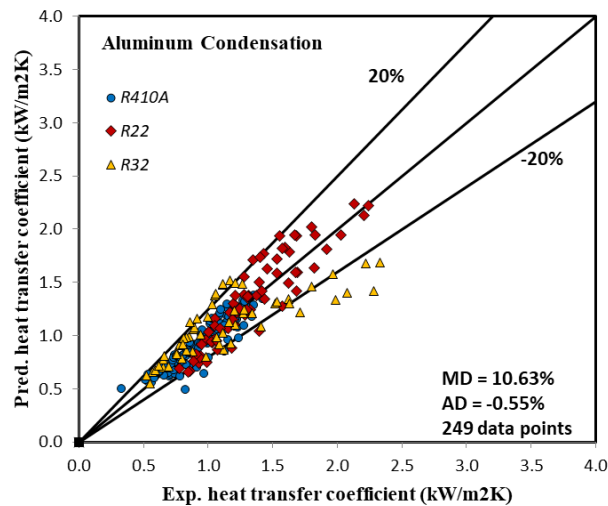


Figure 8: Comparison of predicted and measured values

$$\phi_v^2 = 1 + CX_{tt} + X_{tt}^2 \quad (8)$$

The Lockhart-Martinelli parameter is obtained as the equation (9):

$$X_{tt} = \left(\frac{1-x}{x} \right)^{0.9} \left(\frac{\rho_v}{\rho_l} \right)^{0.5} \left(\frac{\mu_l}{\mu_g} \right)^{0.1} \quad (9)$$

C is a dimensionless parameter adjusted by the least-squares method proposed by (Rahman, Kariya, & Miyara, 2017)

$$C = \lambda x^{0.35} (1-x)^{0.25} \left(\frac{p}{p_{crit}} \right)^{0.31} Re_{tp}^{0.09} We_{tp}^{0.09} \quad (10)$$

where λ is the value depending on the channel geometry and was proposed by Shah and London (R. K. Shah & London, 1978) as:

$$\lambda = 24 \left(1 - 1.355\beta + 1.947\beta^2 - 1.701\beta^3 + 0.956\beta^4 - 0.254\beta^5 \right) \quad (11)$$

where β is the aspect ratio of the channel. The Webb number is obtained from the equation (12):

$$We_{tp} = \frac{G^2 d}{\rho_p \sigma}; Re_{tp} = \frac{Gd}{\mu_{tp}} \quad (12)$$

The comparison between the experimental data and the new correlation is depicted in Fig. 8. The proposed heat transfer coefficient correlation has been validated with 249 data points over the range of mass flux from 50 kg m⁻²s⁻¹ to 500 kg.m⁻²s⁻¹, and the heat flux ranges from 3 kW.m⁻² to 15 kW.m⁻² of R410A, R32 and R22 inside a multiport mini-channel tube. The proposed correlation showed a good agreement with the measured data with a mean deviation of 10.63%.

5. CONCLUSION

The condensation heat transfer of R410A, R32, and R22 in a multiport mini-channel tube was performed in this study. The results are summarized as follows:

- The heat transfer coefficient increases with the increasing of vapor quality, mass flux, and heat flux.
- The heat transfer coefficients of R22 are higher than those of R410A and R32. The main reason is the different thermodynamic properties of refrigerants.

- A new correlation was developed based on the experimental data with the mean and average deviations of 10.63 and -0.55%, respectively.

NOMENCLATURE

A	area	(m ²)
Bo	Bond number	(-)
C	dimensionless parameter	(-)
d	diameter of tube	(mm)
h	heat transfer coefficient	(kW/m ² k)
Pr	Prandtl number	(-)
Re	Reynolds number	(-)
We	Webb number	(-)
Xtt	Lockhart-Martinelli parameter	(-)
x	Vapor quality	(-)

Subscript

<i>internal</i>	internal tube
<i>external</i>	external tube
<i>eq</i>	equivalent
<i>l</i>	liquid
<i>v</i>	vapor
<i>crit</i>	critical
<i>tp</i>	two-phase

ACKNOWLEDGEMENT

This research was supported by Basic Science Research Program through the National Research Foundation of Korea (NRF) funded by Ministry of Education, Science, and Technology (NRF-2016R1D1A1A09919697).

REFERENCES

- Jige, D., Inoue, N., & Koyama, S. (2016). Condensation of refrigerants in a multiport tube with rectangular minichannels. *International Journal of Refrigeration*, 67, 202–213. <https://doi.org/10.1016/j.ijrefrig.2016.03.020>
- Liu, N., & Li, J. (2016). Experimental study on pressure drop of R32, R152a and R22 during condensation in horizontal minichannels. *Experimental Thermal and Fluid Science*, 71, 14–24. <https://doi.org/10.1016/j.expthermflusci.2015.10.013>
- López-Belchí, A., & Illán-Gómez, F. (2017). Evaluation of a condenser based on mini-channels technology working with R410A and R32. Experimental data and performance estimate. <https://doi.org/10.1016/j.apenergy.2017.05.122>
- López-Belchí, A., Illán-Gómez, F., García Cascales, J. R., & Vera García, F. (2016). R32 and R410A condensation heat transfer coefficient and pressure drop within minichannel multiport tube. Experimental technique and measurements. *Applied Thermal Engineering*, 105, 118–131. <https://doi.org/10.1016/j.applthermaleng.2016.05.143>
- Moffat, R. J. (1988). Describing the uncertainties in experimental results. *Experimental Thermal and Fluid Science*, 1(1), 3–17. [https://doi.org/10.1016/0894-1777\(88\)90043-X](https://doi.org/10.1016/0894-1777(88)90043-X)
- Park, J. E., Vakili-Farahani, F., Consolini, L., & Thome, J. R. (2011). Experimental study on condensation heat transfer in vertical minichannels for new refrigerant R1234ze(E) versus R134a and R236fa. *Experimental Thermal and Fluid Science*, 35(3), 442–454. <https://doi.org/10.1016/j.expthermflusci.2010.11.006>
- Pham, Q. V., Choi, K.-I., Oh, J.-T., & Cho, H. (2017). An Experimental Investigation of Condensation Heat Transfer Coefficients and Pressure Drops of Refrigerants Inside Multiport Mini-channel Tubes. *International Journal of Air-Conditioning and Refrigeration*, 25(2), 1750013. <https://doi.org/10.1142/S2010132517500134>
- Rahman, M. M., Kariya, K., & Miyara, A. (2017). Comparison and development of new correlation for adiabatic

- two-phase pressure drop of refrigerant flowing inside a multiport minichannel with and without fins. *International Journal of Refrigeration*, 82(2), 119–129. <https://doi.org/10.1016/j.ijrefrig.2017.06.001>
- Shah, M. M. (2016). Comprehensive correlations for heat transfer during condensation in conventional and mini/micro channels in all orientations. *International Journal of Refrigeration*, 67, 22–41. <https://doi.org/10.1016/j.ijrefrig.2016.03.014>
- Shah, R. K., & London, A. L. (1978). *Laminar Flow Forced Convection in Ducts: A Source Book for Compact Heat Exchanger Analytical Data*.
- Wang, H. S., & Rose, J. W. (2005). A Theory of Film Condensation in Horizontal Noncircular Section Microchannels. *Journal of Heat Transfer*, 127(10), 1096. <https://doi.org/10.1115/1.2033905>
- Zhang, H. Y., Li, J. M., Liu, N., & Wang, B. X. (2012). Experimental investigation of condensation heat transfer and pressure drop of R22, R410A and R407C in mini-tubes. *International Journal of Heat and Mass Transfer*, 55(13–14), 3522–3532. <https://doi.org/10.1016/j.ijheatmasstransfer.2012.03.012>